4-4-2016

The Response of Runoff and Sediment Loading in the Apalachicola River, Florida to Climate and Land Use Land Cover Change

Paige A. Hovenga

Dingbao Wang

Stephen C. Medeiros

Scott C. Hagen

Karim Alizad
University of South Carolina, alizad@sc.edu

Publication Info

Published in *Earth's Future*, Volume 4, Issue 5, 2016, pages 124-142.

AGU PUBLICATIONS

Earth's Future

RESEARCH ARTICLE
10.1002/2015EF000348

Special Section:
Integrated field analysis & modeling of the coastal dynamics of sea level rise in the northern Gulf of Mexico

The response of runoff and sediment loading in the Apalachicola River, Florida to climate and land use land cover change

Paige A. Hovenga[1], Dingbao Wang[1], Stephen C. Medeiros[1], Scott C. Hagen[2], and Karim Alizad[1]

[1]Department of Civil, Environmental, and Construction Engineering, University of Central Florida, Orlando, Florida, USA, [2]Department of Civil & Environmental Engineering, Center for Computation & Technology, Louisiana State University, Baton Rouge, Louisiana, USA

Key Points:
- Prepare future projected climate and land use land cover data including downscaling approach
- Assess runoff and sediment response to changes in climate, LULC, and coupled climate/LULC
- Provide inputs for hydrodynamic and ecological models in the Apalachicola Bay

Corresponding author:
D. Wang, dingbao.wang@ucf.edu

Citation:
Hovenga, P. A., D. Wang, S. C. Medeiros, S. C. Hagen, and K. Alizad (2016), The response of runoff and sediment loading in the Apalachicola River, Florida to climate and land use land cover change, *Earth's Future*, *4*, 124–142, doi:10.1002/2015EF000348.

Received 22 DEC 2015
Accepted 29 MAR 2016
Accepted article online 4 APR 2016
Published online 2 MAY 2016

Abstract The response of runoff and sediment loading in the Apalachicola River under projected climate change scenarios and land use land cover (LULC) change is evaluated. A hydrologic model using the Soil and Water Assessment Tool was developed for the Apalachicola region to simulate daily runoff and sediment load under present (circa 2000) and future conditions (2100) to understand how parameters respond over a seasonal time frame to changes in climate, LULC, and coupled climate/LULC. The Long Ashton Research Station-Weather Generator was used to downscale temperature and precipitation from three general circulation models, each under Intergovernmental Panel on Climate Change (IPCC) carbon emission scenarios A2, A1B, and B1. Projected 2100 LULC data provided by the United States Geological Survey (USGS) Earth Resources Observation and Science (EROS) Center was incorporated for each corresponding IPCC scenario. Results indicate that climate change may induce seasonal shifts to both runoff and sediment loading. Changes in LULC showed that more sediment load was associated with increased agriculture and urban areas and decreased forested regions. A nonlinear response for both runoff and sediment loading was observed by coupling climate and LULC change, suggesting that both should be incorporated into hydrologic models when studying the future conditions. The outcomes from this research can be used to better guide management practices and mitigation strategies.

1. Introduction

Climate change and the consequent long-term effects at both global and local scales have come to the forefront in the scientific, political, and public communities. Natural and human drivers of climate change include increased carbon dioxide (CO_2) concentrations attributed in large to fossil fuel use and changes in land use while agriculture has been principally accredited for the increase in methane and nitrous oxide [*Intergovernmental Panel on Climate Change*, 2013]. Climate change is typically characterized by shifts in temperature and precipitation. The response to it is region specific and includes alteration of extremes, intensities, frequencies, spatial distributions, and temporal patterns [*Karl and Knight*, 1998; *Easterling et al.*, 2000; *Hay et al.*, 2011; *Pal et al.*, 2013; *Wang et al.*, 2013; *National Climate Assessment*, 2014]. These changes impact the hydrologic cycle and have broad implications for fresh water resources in terms of water quantity, e.g., streamflow and quality, e.g., sediment and nutrient loading [*Milly et al.*, 2008; *Wang and Hejazi*, 2011].

In addition to climate change, land cover is altered progressively and abruptly as a result of socio-economic and biophysical drivers that are directed by human-environment conditions [*Lambin et al.*, 2001]. Because land types differ in physical and chemical properties, alterations as land classes expand, migrate, or change entirely can have an impactful influence on freshwater quantity and quality. While previous research on the effects of land use changes on hydrologic processes exists, many focus on historical land changes with interests typically isolated to water quantity or quality; those that do assess future conditions are often specialized and limited by the land class changes that are imposed, e.g., only urban development [*Asselman et al.*, 2003; *Shi et al.*, 2007; *Schilling et al.*, 2008; *Ward et al.*, 2009; *Schilling et al.*, 2010; *Johnson et al.*, 2012].

This study focuses on impacts of climate and land use change on water quantity and quality in the Apalachicola River Basin in Florida using the Soil and Water Assessment Tool (SWAT). Many studies have incorporated climate projections from regional climate models (RCMs) or downscaled general circulation models (GCMs) into hydrologic models including SWAT for this purpose [*Phan et al.*, 2011; *Narsimlu et al.*,

2013; *Shrestha et al.*, 2013; *Jha and Gassman*, 2014]. In addition, SWAT has been used to assimilate land use change and the coupling of climate and land use change for hydrologic modeling studies [*Chen et al.*, 2005; *Schilling et al.*, 2008; *Semadeni-Davies et al.*, 2008; *Park et al.*, 2011; *Yan et al.*, 2013]. Depending on the study, climate versus land use change impacts have been found to be more significant than the other and changes in one may amplify the effects of the other [*Praskievicz and Chang*, 2009].

For the Apalachicola region, *Chen et al.* [2014] evaluated both seasonal and event scale responses of runoff and sediment loads using climatic data from two RCMs (HRM3-HADCM3 and RCM3-GFDL). Seasonal response was slight with contrasting behavior produced from the individual models. At the event scale, flow increased from the baseline by 8% for HRM3-HADCM3 and 50% for RCM3-GFDL. Research by *Johnson et al.* [2012], *Johnson et al.* [2015], and *U.S. Environmental Protection Agency* [2013] investigated the sensitivity of streamflow and water quality in the Apalachicola-Chattahoochee-Flint (ACF) River Basin to mid-century climate change from four GCMs, downscaling methodology, i.e., no downscaling, statistical, and dynamical, and to urban/residential development. Sensitivity of flow (both average and extreme) and sediment loading differed in response to climate change among the climate models and downscaling approaches used. While changes in climate induced both increases and decreases in flow, sediment loading increased overall. Climate was also determined more impactful than urban development at the large-scale simulation. *Gibson et al.* [2005] focused on flow regime (magnitude, duration, frequency, timing, and rate of change) under climate change and projected human demand. Decreased flow variability and lower high and low flows were reported. While response among varying GCMs has been assessed, previous studies for Apalachicola have limited climate change to one IPCC Special Report on Emission Scenarios (SRES) scenario. The SRES scenarios represent future carbon emissions of equally probable outcome resulting from a range of driving forces (e.g., social, economic, environmental, and technologic) [*Intergovernmental Panel on Climate Change*, 2000]. The variability within GCMs among equally likely scenario outputs has not previously been explored. In addition, land use land cover (LULC) studies have focused singularly on anthropogenic changes, and the ways in which the region will respond to comprehensive LULC change have not been addressed. The individual and interrelated ways the aforementioned drivers, i.e., climate change from individual GCMs and comprehensive LULC change, both within the context of SRES scenarios, may affect overland processes in the Apalachicola region is needed.

The objective of the research developed herein was to assess the isolated and coupled impacts of climate change and LULC change using a comprehensive platform guided by the IPCC SRES [*IPCC*, 2000]. A SWAT model developed for the Apalachicola River region was used to simulate runoff and sediment loading under present and future conditions. Downscaled climate data for three GCMs and LULC projections, detailing changes for 16 distinct land classes, are both characterized by the SRES scenarios A2, A1B, and B1 for 2100 [*IPCC*, 2000]. In using IPCC SRES correlated data, the forcing factors that drive climate change align with those that drive LULC change, providing a congruent foundation from which inter-comparisons can be made. The suite of plausible, potential responses can be used for climate change assessments including those related to the ecology and potential sea level rise (SLR) impacts, as well as to inform and guide management strategies.

Apalachicola is a fluvial-driven estuarine system. As such, SLR resulting from climate change may increase the coastal vulnerability of the region [*National Climate Assessment*, 2014] with respect to the ecology, hydrodynamics [*Bilskie et al.*, 2016; *Passeri et al.*, 2016], and geomorphology [*Plant et al.*, 2016]. Previous research has shown that tidal flows and storm surge dynamics in Apalachicola Bay will be altered under future SLR [*Bilskie et al.*, 2016; *Passeri et al.*, 2016]. Further, SLR coupled with river inflow may induce changes in residual circulation intensities, peak stage and flow, and marsh production [*Martin et al.*, 2002; *Sathiamurthy*, 2013; *Valentim et al.*, 2013]. To understand, maintain, and enhance resiliency, an analysis of the coastal dynamics of SLR must implement an integrated approach that accounts for changes not only in hydrodynamics but also in the hydrologic cycle [*Passeri et al.*, 2015]. This study addresses the effects of climate change on overland processes, river inflow, and sediment loading for the Apalachicola region, an integral component for climate change vulnerability assessments as well as coastal management decision making.

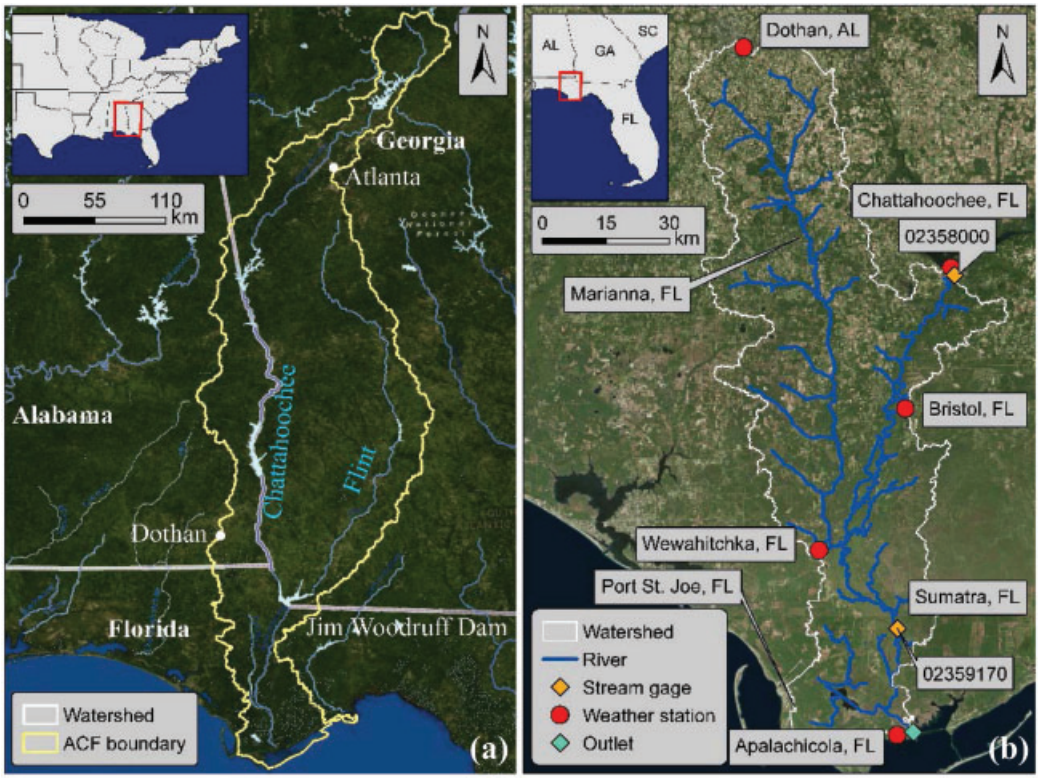

Figure 1. (a) Apalachicola-Chattahoochee-Flint (ACF) River Basin shown by the yellow boundary and the study domain indicated by the white boundary; and (b) the study domain in more detail.

2. Study Domain

Located in the southeastern United States, the ACF River Basin extends to north Georgia, includes southeast Alabama, and covers part of Florida's Panhandle as shown by the yellow boundary in Figure 1a. The Flint and Chattahoochee Rivers converge at Lake Seminole near the Florida-Georgia state line. The Jim Woodruff Lock and Dam marks the beginning of the Apalachicola River, a meandering river with extensive floodplains. Flowing to the south, it ultimately discharges to the shallow, estuarine Apalachicola Bay in the Northern Gulf of Mexico.

This study focuses on the southern portion of the ACF River Basin indicated in Figure 1a and in more detail in Figure 1b. It includes the Apalachicola River, beginning in the north at the Jim Woodruff Lock and Dam near Chattahoochee, Florida and extends south to the bay. The tributary to the west, the Chipola River, is also included and stretches to the north as far as Dothan, Alabama. The entire watershed study area is 575,930 ha. Developed regions included in the domain, aside from Chattahoochee and Dothan, are Marianna, Bristol, Wewahitchka, Sumatra, Port St. Joe, and Apalachicola, Florida

The Apalachicola River Basin has a subtropical, humid climate, with low temperatures in January varying from 4°C to 13°C and high temperatures vary from 24°C to 27°C in July [*Couch et al.*, 1996]. Average annual rainfall is approximately 1500 mm, though there is an uneven distribution with regions to the west of the river receiving one-third less rainfall that those to the east [*Livingston*, 1984]. Seasonally there are two peaks, one in March and another occurring in late summer/early fall from July to September.

The Apalachicola River has the largest discharge of all rivers in Florida and is ranked 21st in magnitude within the conterminous United States. The average annual discharge from 1978 to 2012 was 680 cm^3/s with fluctuations ranging from 283 to 1048 cm^3/s [*United States Geological Survey*, 2012]. Sediment deposition rates for the Apalachicola system are greater than other estuaries in the Gulf Coast with relatively high sand content and low silt content. Samples from 1825 to 1900 indicate that silt was more prevalent in this system historically and while the quantity of sediment delivered to the bay has remained unchanged since the

1950s, it is suggested that the abrupt changes in the sediment regime may be caused by anthropogenic factors such as the implementation of dams [*Isphording*, 1986].

Significant to both the ecology and economy, the coastal estuarine system provides a habitat for many types of flora and fauna including salt marshes, seagrasses, and oyster beds. Salt marshes and seagrasses provide shelter and reproductive grounds for many terrestrial and aquatic species. Oysters are highly productive in this region and provide over 90% of Florida's and 8–10% of the nation's oysters [*Livingston*, 1984]. Previous studies have found changes in climate and LULC may affect both streamflow and sediment loading by altering peaks and total quantities associated with extreme events, resulting in increases and decreases at the seasonal scale, shifts in flow variability, and amplification of both attributes [*Gibson et al.*, 2005; *Praskievicz and Chang*, 2009; *Johnson et al.*, 2012; *Chen et al.*, 2014]. To better adapt to and mitigate adverse effects of climate and LULC changes for this region, a comprehensive assessment and understanding of the response of runoff and sediment to the aforementioned changes are required.

3. Methodology

The purpose of this study was to assess how runoff and sediment respond to climate and LULC changes in the Apalachicola River. To do so, a hydrologic model was developed, calibrated, and validated for historical conditions (1984–1994). The model was then used to simulate 30 years of daily discharge and sediment load under present (circa 2000) and future (2100) conditions. Future scenarios incorporated changes in climate, LULC, and coupled climate and LULC. Hydrologic responses in terms of monthly averages of runoff and sediment loading were assessed.

3.1. Hydrologic Model Development

The hydrologic model selected for this study was the SWAT, a physically based, continuous time model designed to simulate long-term hydrologic processes within large watersheds [*Srinivasan and Arnold*, 1994; *Neitsch et al.*, 2011]. SWAT is an open source model capable of simulating both water quantity and quality on daily or coarser time scales and has been extensively used in hydrologic studies including those that assess climate and LULC change impacts [*Gassman et al.*, 2007; *Johnson et al.*, 2012; *Zhang et al.*, 2013; *Wang et al.*, 2014; *Krysanova and Srinivasan*, 2015]. The most recent release available when the study first commenced (SWAT2012.10_1.8) was used. SWAT simulates surface runoff using the Soil Conservation Service (SCS) curve number procedure [Soil Conservation Service, 1972], and evapotranspiration was calculated using the Penman-Monteith method [*Monteith*, 1965]. Sediment yield was computed from the Modified Universal Soil Loss Equation (MUSLE) and a simplified Bagnold equation was used to model sediment routing [*Williams*, 1995].

Model inputs included spatially distributed LULC data, elevation, and soil maps. LULC data for 1992 was obtained from the National Land Cover Database (NLCD) [*Vogelmann et al.*, 2001]. The digital elevation model (DEM) was derived from online accessible, topographic data provided by the Northwest Florida Water Management District (http://www.nwfwmdlidar.com/) and surveyed bathymetry provided by the U.S. Army Corps of Engineers, Mobile District. At 5 m resolution, the extent spanned from the bay to as far north as Marianna, Florida. For the remaining part of the basin, 1/3″ (~10 m) resolution data obtained from the National Elevation Dataset (NED) were used [*United States Geological Survey*, 2013a]. The soil map was acquired from the Soil Survey Geographic Database (SSURGO) [*United States Department of Agriculture*, 2007]. The 5760 km^2 watershed was comprised of 13 hydrologic unit code at the 10 digit spatial scale [*Seaber et al.*, 1987; *United States Geological Survey*, 2013b]. It was delineated into 99 subbasins that were then further broken into a total of 4187 hydrological response units for which the land use, topography, soil type, and management practices may be assumed relatively homogeneous.

Typical climatic data inputs for SWAT include precipitation, temperature, solar radiation, relative humidity, and wind speed. Observed daily data can be used singularly or in conjunction with a weather generator. The National Centers for Environmental Prediction (NCEP) developed the Climate Forecast System Reanalysis (CFSR) that provides weather data in the SWAT file format [*National Centers for Environmental Prediction*, 2016]. Values from CFSR were generated for missing daily rainfall and temperature data and for all other climatic variables. Climatic data (precipitation and temperature) were downloaded for five stations, shown in Figure 1b, from the National Centers for Environmental Information (NCEI) for 1984–1994 [*Menne et al.*, 2012]. This period will henceforth be referred to as the "historic" period.

The model employed one boundary condition for daily streamflow and sediment loading at the Jim Woodruff Lock and Dam. The boundary was applied at the same location as the United States Geological Survey (USGS) station (02358000) and is shown in Figure 1b [*United States Geological Survey*, 2001]. Observed daily streamflow and sediment load data were downloaded from the USGS station. Because of the limited number of observed sediment records occurring within the historic period, a power law regression analysis was performed between the observed, daily streamflow, and sediment load to establish a relationship that was used to derive an empirical sediment load. Sediment rating curves in the power function form are commonly used to estimate suspended sediment in rivers by relating observed discharge and sediment [*Walling*, 1974; *Asselman*, 2000; *Tóth and Bódis*, 2015]. Observed daily values for streamflow and sediment load were also downloaded for a USGS station near Sumatra, Florida (02359170) and used for the model calibration and validation (Figure 1b).

3.2. Projected Climate Change

Climate change projections referred to the IPCC Fourth Assessment Report (AR4), which was the most recent assessment report available at the commencement of this study [*Intergovernmental Panel on Climate Change*, 2007]. Improvements have since been made to climate models used in the most recent Fifth Assessment Report (AR5), yet, there is overall consistency for large-scale patterns between the AR4 and AR5 projections [*Intergovernmental Panel on Climate Change*, 2014b]. Future conditions impose A2, A1B, and B1 scenarios from the IPCC SRES [*IPCC*, 2000]. The AR4 utilizes a linear process whereby the SRES storylines are used to create carbon emission scenarios; emissions are applied within climate models to assess impacts. The process differs from that used in the AR5, which uses trajectories of radiative forcing levels called representative concentration pathways (RCPs) [*Intergovernmental Panel on Climate Change*, 2014a]. RCPs are representative of both climate and socio-economic scenarios, which are developed in parallel.

The SRES A2 scenario describes a heterogeneous world with uneven economic and technological growth and diversified social and political constructs. A1B describes a rapidly changing world with economic growth, population increase that then declines by 2100, and balance between supply sources and technological advancements. B1 is similar to A1B, describing a rapidly changing world with economic balance but differs in that social and technological advancement is geared toward environmental conservation and sustainability. When developing the SRES scenarios, four world regions referred to as "macro-regions" were aggregated for modeling purposes. This study area is part of the Organization for Economic Cooperation and Development (OECD90) Region which is considered an industrialized country (IND). The 2100 A2, A1B, and B1 population growth (billions) for IND is about 2.2, 1.4, and 1.4 and the economic growth (gross domestic product) is around 2.3, 2.9, and 2.5, respectively [*IPCC*, 2000]. The total CO_2 emissions (gigatonnes carbon) including fossil and land use for the A2, A1B, and B1 scenarios in the OECD90 Region is 6.91, 2.25, and 0.99, respectively [*IPCC*, 2000]. Fully described storylines, details on global and region-specific socio-economic drivers, and data for each emission scenario are provided in the SRES [*IPCC*, 2000].

Structural differences between GCMs can result in contradictory climate predictions at local scales [*Semenov and Stratonovitch*, 2010]. Further, specific GCMs have been shown to perform better for particular regions. *Cai et al.* [2009] assessed the performance of 17 GCMs based on hindcasts of temperature and precipitation. Skill scores, based on the root mean square error for each GCM and ranging from 0.00–0.06, 0.06–0.10, 0.10–0.20 to >0.20, were plotted globally on a $2° \times 2°$ grid. The average skill score was 1/17 or about 0.06. A skill score <0.06 indicated that the GCM performed less than average, and a skill score >0.06 indicated that the GCM performed above average. The skill score as well as the model data availability for precipitation and temperature to incorporate the maximum number of carbon emission scenarios guided the GCM selection process for this study. For a comprehensive assessment and to better capture uncertainty, a multi-model approach was taken. The following three models were ultimately selected: (1) HadCM3 (HADCM3), (2) IPSL-CM4 (IPCM4), and (3) ECHAM5-OM (MPEH5) [*Semenov and Stratonovitch*, 2010]. The temperature skill score for each of the models fell within the 0.06–0.10 range. The precipitation skill score for IPCM4 and MPEH5 was 0.06–0.10 while for HADCM3 ranged 0.10–0.20. The skill scores indicate that the selected GCMs perform above average for the study region.

Because of their coarse resolution, GCMs generally struggle to capture small-scale processes that occur at local extents which can result in inaccurate predictions for models at those scales. Moreover, GCMs often provide monthly averages or change rates, while many process-based models, including SWAT, require daily

inputs. Various temporal and spatial downscaling techniques have been developed to resolve these issues including the implementation of neural networks, bias-correction and spatial downscaling, regressions, and weather generators. Statistical downscaling techniques produce relatively quick results and are computationally inexpensive, however, a disadvantage is the assumed constant empirical relationships [*Mearns et al.*, 2004]. The issue of non-stationarity may be resolved using a stochastic approach [*Richardson*, 1981; *Wilby*, 1997]. Stochastic weather generators have been shown to outperform alternative statistical downscaling methods for general circulation models at the single site level [*Wilby et al.*, 1996; *Wilby and Wigley*, 1997].

For this study, the Long Ashton Research Station-Weather Generator (LARS-WG) was selected for downscaling GCM data because of its ability to generate site specific, daily, stochastic temperature and precipitation [*Semenov and Stratonovitch*, 2010]. LARS-WG has been used in a number of studies to develop and assess climate change scenarios [*Semenov and Barrow*, 1997; *Dibike and Coulibaly*, 2005; *Ogdena et al.*, 2006; *Ficklin et al.*, 2009] and has been shown to perform well in subtropical climates of the southeast United States [*Semenov et al.*, 1998]. LARS-WG is capable of producing daily, synthetic weather time series, i.e., baseline, developed from and having the same statistical characteristics as localized, observed daily data. Similarly, future synthetic data can be generated for each carbon emission scenario, e.g., A2, and time period, e.g., 2081–2100, as predicted by the GCMs. Predictions from 15 GCMs used in the AR4 have been built into the newest version of LARS-WG. Computed monthly changes between the baseline scenario and future synthetic projections are incorporated into a scenario file (.sce) that is used by LARS-WG to perturb the baseline parameters, i.e., minimum/maximum temperatures, rainfall, and solar radiation, at each grid point. Data are interpolated across the study area between grid points using local and global interpolation procedures [*Semenov and Brooks*, 1999]. The final downscaled, daily climate data for temperature and rainfall are provided at each location for which the observed data was provided. Because of the limited historical data available for the study region, projected solar radiation was not included in the climate change assessments.

Thirty years of observed data, 1970–1999, from the above-mentioned five weather stations previously shown in Figure 1b were used to create the baseline scenario representative of present day conditions. Weather was then generated under 2100 carbon emission scenarios (A2, A1B, and B1) as predicted by the GCMs (HADCM3, IPCM4, and MPEH5). The relative monthly change in precipitation and the absolute monthly change in temperature for each scenario were incorporated into a scenario file and the resulting outputs from LARS-WG provided the downscaled 2100 weather data used by SWAT.

3.3. Projected LULC Change

Historical changes in LULC for the Apalachicola region have been studied by *Pan et al.* [2013]. From 1985 to 2005, the growth rate of urban areas was 79% and was typically converted from forest/woody wetland. From 1985 to 1996, shrub and barren land decreased. Forest/woody wetland also increased during this period before declining from 1996 to 2005 as a result of increased cropland/pasture from 1996 to 2005. In keeping with the IPCC carbon emission scenarios, projected 2100 A2, A1B, and B1 LULC provided by the USGS EROS Center was selected to assess LULC change impacts [*USGS EROS Center*, 2014]. Maps were developed using historical land cover change, global integrated assessment model data, and expert analysis to downscale SRES narratives to national and sub-national scales [*USGS EROS Center*, 2014]. Some land cover classes in the 2100 LULC were incongruent with those recognized by SWAT in the land cover lookup tables and were therefore adapted in a way that the datasets could be incorporated into the SWAT model and were comparable with present day classifications.

From present to 2100, A2, forests yield to agriculture, a 109% increase, and urban areas, particularly Dothan, Alabama, Marianna, Wewahitchka, Port St. Joe, and Apalachicola, Florida, are predicted to increase. A1B has an increase in urban area with less emphasis near the coast and less new agricultural area as compared with A2. B1 has similar urban development as A1B, however, there is a 31% decrease in agricultural area as it gives way to forested area. From circa 2000 to 2100, wetlands, both forested and non-forested, remain fairly consistent.

3.4. Model Performance

The Nash-Sutcliffe efficiency (NSE) and percent bias (PBIAS) were used to measure the model's performance of daily output for the calibration and validation periods, with optimal scores being equal

Table 1. Summary of Evaluation Metrics

	NSE	PBIAS
Evaluation metrics	• NSE = 1 optimum • 0 < NSE < 1 model predictions more accurate than mean of measured data • NSE = 0 model predictions as accurate as mean of measured data • NSE < 0 mean of measured data more accurate than model predictions	• PBIAS = 0 optimum • PBIAS > 0 indicates model under prediction bias • PBIAS < 0 indicates model over prediction bias

NSE, Nash-Sutcliffe efficiency; PBIAS, percent bias.

to 1 and 0, respectively. The NSE measures the residual variance to the variance of the observed data:

$$\mathrm{NSE} = 1 - \frac{\sum_{i=1}^{n} \left(X_i^{\mathrm{obs}} - X_i^{\mathrm{sim}}\right)^2}{\sum_{i=1}^{n} \left(X_i^{\mathrm{obs}} - \overline{X^{\mathrm{obs}}}\right)^2} \quad (1)$$

where X_i^{obs} was the ith observation for the constituent being evaluated, X_i^{sim} was the ith simulated value for the constituent being evaluated, and $\overline{X^{\mathrm{obs}}}$ was the mean of the observations for the constituent being evaluated. An NSE equal to zero indicated the model predictions were as accurate as the measured data average and less than zero indicated the mean of the observed data was a better predictor than the model results [*Nash and Sutcliffe*, 1970]. Percent bias measured the model's average tendency to predict higher or lower values than the observed data:

$$\mathrm{PBIAS} = \left[\frac{\sum_{i=1}^{n} \left(X_i^{\mathrm{obs}} - X_i^{\mathrm{sim}}\right) \times 100}{\sum_{i=1}^{n} \left(X_i^{\mathrm{obs}}\right)}\right] \quad (2)$$

A positive PBIAS indicated that the model tends to under predict values and a negative PBIAS indicated a model overestimation bias [*Gupta et al.*, 1999]. A summary of the evaluation metrics are provided in Table 1. The NSE was the primary statistic used during the model calibration and the PBIAS served as a secondary measure.

3.5. Assumptions and Limitations

The U.S. Army Corps of Engineers currently regulates flow from the Jim Woodruff Lock and Dam. In the case of the future scenarios, the boundary conditions of streamflow and sediment load were assumed to remain unchanged from historic conditions. A study of the upper ACF River Basin reported climate change scenarios with 2050 demands resulted in greater magnitude and higher frequency of instream flow target deficits, total water supply deficits, and decrease in energy generation [*Georgakakos et al.*, 2010]. The ACF River Basin is subject to ongoing litigation and boundary conditions at the Jim Woodruff Lock and Dam may change in the future.

In addition, the DEM and soil distributions were assumed to remain constant from circa 2000 to 2100, and channel erosion was not considered for this study. Increases in atmospheric CO_2 concentration were assumed to remain constant at 330 parts per million volume. Increased CO_2 can alter plant stomatal conductance impacting evapotranspiration, though a study by *Butcher et al.* [2014] suggests the offsetting may be overestimated by SWAT. Lastly, the watershed model selection is, in it of itself, a limitation of the study. Discrepancies among different model predictions are attributed equally to differences in the model calibration strategy and structure [*Caldwell et al.*, 2015]. The use of the curve number approach and MUSLE are particular weaknesses of the SWAT model [*Benaman et al.*, 2005].

Table 2. Simulations and Applied Climate/LULC Conditions

Description Conditions	Simulation	Climate (Scenario—GCM)	LULC
Baseline	1	Present (circa 2000)	Present (circa 2000)
Climate only	2	A2—HADCM3	Present (circa 2000)
	3	A1B—HADCM3	
	4	B1—HADCM3	
	5	A2—IPCM4	
	6	A1B—IPCM4	
	7	B1—IPCM4	
	8	A2—MPEH5	
	9	A1B—MPEH5	
	10	B1—MPEH5	
LULC only	11	Present (circa 2000)	2100 A2
	12	Present (circa 2000)	2100 A1B
	13	Present (circa 2000)	2100 B1
Climate and LULC	14	A2—HADCM3	2100 A2
	15	A1B—HADCM3	2100 A1B
	16	B1—HADCM3	2100 B1
	17	A2—IPCM4	2100 A2
	18	A1B—IPCM4	2100 A1B
	19	B1—IPCM4	2100 B1
	20	A2—MPEH5	2100 A2
	21	A1B—MPEH5	2100 A1B
	22	B1—MPEH5	2100 B1

GCM, general circulation models; LULC, land use land cover.

4. Results

In the next section, the model performance for the historical time period (1984–1994) is discussed. Following is the assessment of runoff and sediment response to changes in (1) climate, (2) LULC, and (3) coupled climate and LULC. Results were evaluated at the outlet near the mouth of the river outside the bound of tidal influence prior to entering Apalachicola Bay as indicated in Figure 1b. When assessing the seasonal response of climate and LULC change, streamflow and sediment load that were applied at the Jim Woodruff Lock and Dam boundary were excluded; daily influx values were subtracted from the daily output values at the outlet prior to analysis. This was carried out to further target alterations originating in the study domain and highlight changes that might otherwise be diluted by incorporating the total flow. The baseline simulation represented present day conditions and served as the constant to which the future simulations' predictions were compared.

Table 2 shows the total simulation ensemble detailing the climate and LULC implemented for each. In the case of climate only, data are presented for each carbon emission scenario (A2, A1B, and B1) as predicted by each GCM (HADCM3, IPCM4, and MPEH5); LULC represents present day conditions. There were a total of nine simulations for this category. For the LULC only simulations, climate was representative of present day conditions and 2100 LULC for each carbon scenario was implemented, making for a total of three simulations. Incorporating coupled climate and LULC change, a total of nine simulations captured the carbon scenarios for each GCM and corresponding 2100 LULC.

4.1. Model Calibration and Validation

The model calibration and validation periods were 1985–1989 and 1990–1994, respectively. To reach stable conditions and avoid erroneous outputs, a 1-year ramp-up period was applied, and therefore, results from 1984 were excluded during calibration. A list of the calibrated parameters, their descriptions, and adjusted values are listed in Table 3. The calibration adjustments with percentages described the percent

Table 3. Calibrated SWAT Parameters, Descriptions, and Adjustments

Parameter	Description	Calibration Adjustment
CN2	SCS runoff curve number	−21.0%
CH_N2	Main channel Manning's "*n*"	0.019
CH_K2	Main channel effective hydraulic conductivity (mm/h)	110
ALPHA_BF	Baseflow alpha factor (1/days)	0.25
CH_S2	Main channel average slope (m/m)	+6.0%
ESCO	Soil evaporation compensation factor	0.75
SURLAG	Surface runoff lag coefficient	0.5
GW_DELAY	Groundwater "revap" coefficient	0.2
RCHRG_DP	Deep aquifer percolation factor	0.54
HRU_SLP	Average slope steepness (m/m)	−15.0%
USLE_P	USLE equation support practice factor	0.055
SLSUBBSN	Average slope length (m)	+50.0%
OV_N	Manning's "*n*" for overland flow	+50.0%

SCS, Soil Conservation Service; SWAT, Soil and Water Assessment Tool.

change of the parameter value from the original, default value. A single number reported for the calibration adjustment represented the ultimate value assigned for the parameter within the SWAT model. The model streamflow NSE calibration and validation values were 0.84 and 0.69, respectively. The PBIAS for flow calibration and validation were −2.42 and −9.32, respectively. The sediment NSE was 0.42 and 0.44 and the PBIAS were 15.97 and −29.74, for the calibration and validation periods, respectively. According to the literature and guidelines set by *Moriasi et al.* [2007], the model performance for streamflow and sediment was determined to be above satisfactory, and can be considered good or very good for the application of daily time steps [*Saleh and Du*, 2004; *Singh et al.*, 2005; *Tuppad et al.*, 2011]. The model adequately reproduced baseflow and surface runoff, both in magnitude and timing, and despite difficulties often associated with modeling sediment, seasonal, and event fluctuations were sufficiently captured by the model.

4.2. Response to Climate Change

Using LARS-WG, 30 years of daily, stochastic weather was generated to represent present day (circa 2000) and future (2100) conditions for the A2, A1B, and B1 carbon emission scenarios predicted by the HADCM3, IPCM4, and MPEH5 climate models. The monthly change in relative rainfall and absolute temperature between the baseline and future climate scenarios for each GCM are shown in Figure 2. Among the GCMs, there were stark dissimilarities in the relative change in rainfall. HADCM3 predicted wetter wet seasons and a drier dry season. IPCM4 overall predicted a decrease in rainfall with the exception of August and September. MPEH5 showed an increase in rainfall with the exception of August. The average annual relative change for the HADCM3, IPCM4, and MPEH5 models were 1.04, 0.86, and 1.17, respectively. The relationship among the carbon emission scenarios was sporadic with no one prevailing in more or less relative change to rainfall.

The GCMs agreed that temperature will increase in this region from present to future conditions. HADCM3 had the largest absolute increase, particularly during the dry season. IPCM4 was generally consistent throughout the year with little seasonal fluctuation, and MPEH5 showed a slighter increase for May, June, October, and November. In regard to the carbon scenarios, A2 showed a dominant increase in temperature to the other scenarios. A1B was secondary and the B1, while still showing an increase, was smaller than A2 and A1B.

The average, monthly runoff (cms) and sediment loading (ton/day) were used to compare quantities and seasonal shifts from present (baseline) to future for simulations incorporating climate change (Figure 3). HADCM3 predicted a more heterogeneous seasonal pattern than the baseline, with higher high flows (near January–April and September–November) and lower low flows (May–August). This pattern was closely correlated with the relative change in rainfall (Figure 2a). While changes in precipitation and temperature both impact runoff, they tend to do so in opposite ways that may cancel out the effects of the other [*Butcher*

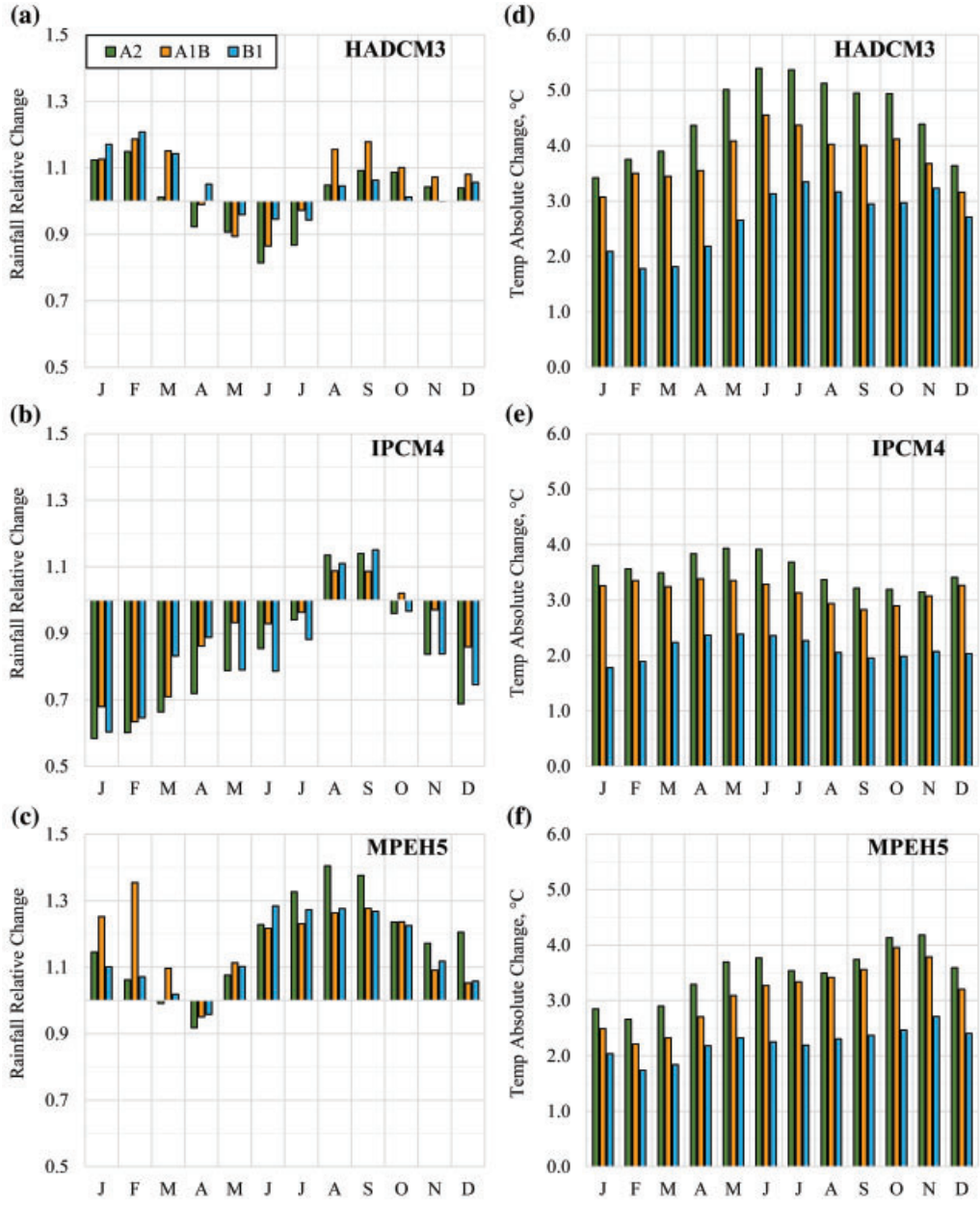

Figure 2. Monthly relative change in rainfall (a) HADCM3, (b) IPCM4, and (c) MPEH5 and absolute change in temperature (°C) (d) HADCM3, (e) IPCM4, and (f) MPEH5 from present to future for the study domain. The colors represent carbon scenarios A2 (green), A1B (orange), and B1 (blue).

et al., 2014]. An example of such behavior occurs in January for the A2 scenario when rainfall and temperature increase; yet, runoff remains nearly unchanged from the baseline. For the majority of the year, the A2 scenario produced lower runoff than A1B and B1. The highest runoff was predicted by B1 during the earlier months of the year (January–July) and then a shift occurred for the later months (August–December) when A1B was highest. Compared with the baseline, future sediment will likely be amplified during high loading periods and decreased during low loading periods. In general, when runoff is predicted to increase or decrease from present to future, sediment mirrors the behavior. The exception to this trend occurred later in the year (August–December) when sediment was predicted to increase despite flow decreases for the A2 and B1 scenarios. The relationship between runoff and sediment was also nonlinear. An example of this was seen for March when A1B estimated a 60% increase in sediment loading relative to a 16% increase in runoff.

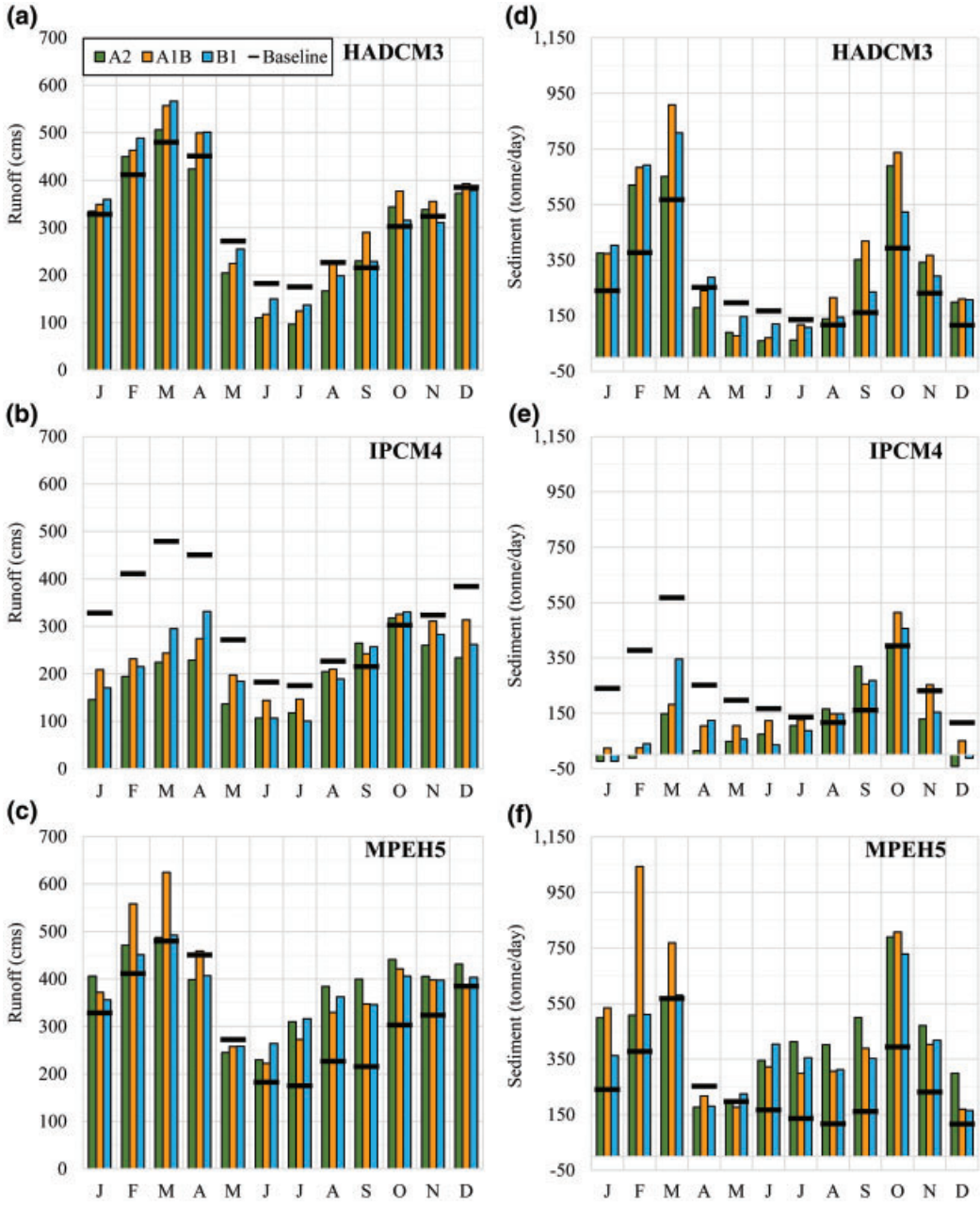

Figure 3. Monthly average runoff (cms) for (a) HADCM3, (b) IPCM4, and (c) MPEH5 and sediment load (ton/day) (d) HADCM3, (e) IPCM4, and (f) MPEH5 at the outlet. The colors represent baseline (black) and carbon scenarios A2 (green), A1B (orange), and B1 (blue). Only climate change is considered.

IPCM4 forecasted a future decrease in runoff for all months and for each carbon scenario, with the exception of September and October (Figure 3b). The average monthly flows were more homogenous throughout the year, similar to the absolute temperature increase for IPCM4, which had smoother seasonal transitions compared with other GCMs (Figure 2e). Patterns emerging between the carbon scenarios were difficult to distinguish, though A1B tended to predict higher flows than A2 and B1 during the drier summer months. Around the wet season from January to May, there was an average percent reduction of 54%, 43%, and 45% from the baseline to future for A2, A1B, and B1 scenarios, respectively. There was also an estimated increase of loading during the months of August–October. Following the flow pattern, higher sediment loading throughout the year was estimated by the A1B scenario compared with A2 and B1.

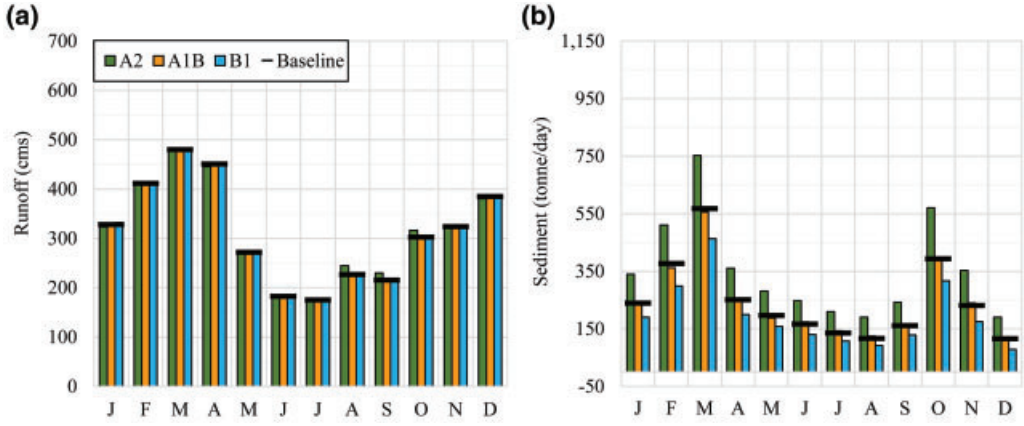

Figure 4. Monthly average (a) runoff (cms) and (b) sediment load (ton/day). The colors represent baseline (black) and carbon scenarios A2 (green), A1B (yellow), and B1 (blue) at the outlet. Only LULC change is considered.

Results using the MPEH5 model indicated that runoff may increase, particularly during later months of the year (June–December), with A2 estimating the largest quantities (Figure 3c). During February and March, A1B was the dominant scenario and increased by 36% and 30%, respectively. In correspondence with this, the sediment loading also drastically increased from 177% to 36% (Figure 3f). Within the wet seasons, the A1B scenario had the largest loadings and during the dry season, A2 was typically largest. Minimum loadings were predicted by the MPEH5 model to occur in April and May.

The dissimilarities in response to climate change as predicted by the GCMs highlighted the structural differences that exist between each model. Still, general trends can be extracted where outputs were in agreement for all the three GCMs. The GCM ensemble converged on runoff and sediment loading increasing in September and October for each scenario. With the enlarged flow, accompanied sediment loading was also increased for these months. Further, loading for the baseline was at its minimum from July to September, however, future minimal values occurred earlier in the year around April to June.

4.3. Response to Land Use Land Cover Change

Present to future quantities and seasonal shifts in average, monthly runoff (cms) and sediment loading (ton/day) to changes in LULC were compared (Figure 4). Runoff was virtually unaltered by the changes made to land use; future quantities matched the present baseline with monthly differences equaling no more than ±20 cms, occurring from August to October. Sediment loading was more affected with monthly averages differing from the baseline ±185 ton/day (Figure 4b). Further, a distinct response to the specific carbon emission scenarios was more easily identifiable. The A2 scenario predicted an increase in loading for all months. The largest increase of 33% occurred in March. A1B produced similar monthly averages compared to the baseline, and B1 resulted in a decrease in sediment loading. The largest deviation between the baseline and B1 also occurred in March, when the sediment loading was projected to reduce by 18%. Over the course of the entire 30-year simulation, the sediment percent change for A2, A1B, and B1 from the baseline were +43.8%, −0.4%, and −20.8%, respectively, while the percent change for runoff was less than 1% for all the scenarios. In general, the seasonal fluctuations of future runoff and sediment loading remained consistent with present day conditions.

4.4. Response to Coupled Climate and Land Use Land Cover Change

The coupling of both future climate and LULC change was simulated for each GCM. The general behaviors of increasing or decreasing from the baseline to the future for monthly average runoff and sediment loading were analogous to the climate only simulation results. Similar to the climate only simulations, climate plus LULC change produced a large gradation in the outputs produced by different GCMs. That is, the HADCM3 model predicted higher high flows and lower low flows, IPCM4 indicated overall lowered runoff, and MPEH5 produced generally increased flow. The general seasonal behaviors for sediment loading were also very similar to the climate only simulation results.

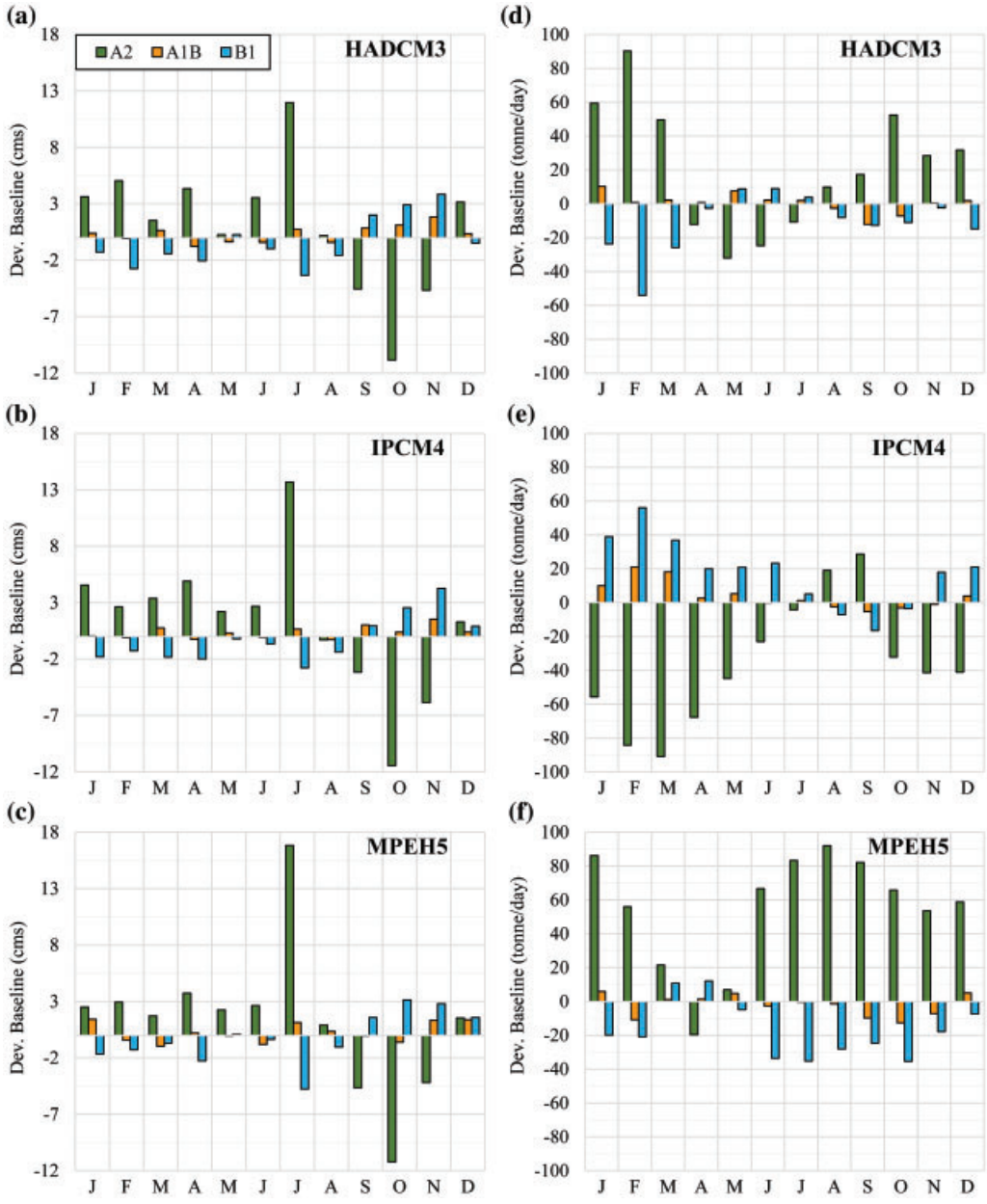

Figure 5. Climate and land use land cover (LULC) deviations — (climate only deviations + LULC only deviations) for the monthly average runoff (cms) for (a) HADCM3, (b) IPCM4, and (c) MPEH5 and sediment load (ton/day) for (d) HADCM3, (e) IPCM4, and (f) MPEH5 at the outlet. The colors represent carbon scenarios A2 (green), A1B (yellow), and B1 (blue).

Therefore, the coupled climate and LULC change simulations were used to test if the simulated response might be represented by modeling these processes as isolated occurrences and then, estimated using the method of superposition or if the interaction between climate and LULC change resulted in a dynamic response. To do so, runoff and sediment loading deviations from the baseline to the future for climate only, LULC only, and coupled climate and LULC were computed for all carbon emission scenarios predicted by each GCM. The additive deviation quantities for the climate only and LULC only simulations were then subtracted from the coupled climate and LULC simulation deviations for both runoff and sediment load (Figure 5). A value of zero in Figure 5 represents a linear response. A value greater than zero in the figure indicates a dynamic response where deviations from the baseline, regardless of being an increase or decrease, would be larger by incorporating climate and LULC simultaneously in the model than predicted

using the additive deviations for the individual responses. A values less than zero still indicates a dynamic response but one where the coupled climate and LULC change simulation predicted less of a deviation from the baseline for future conditions than would be estimated by superimposing the individual processes.

Figures 5a–5c show the monthly average runoff response with near zero, positive, and negative values for the carbon emission scenarios that were similar among the three GCMs. The A2 scenario indicated the coupling effect of climate and LULC changes may result in an amplified response for the months of December–July while a dampened response was observed for August–November. A near polar response to the monthly behavior displayed by A2 was detected for the B1 scenario, while A1B was relatively close to zero, differing no more than ±2 cms. Overall, the modeled response of runoff to the coupling of climate and LULC change was minimal, with differences between that versus the summated values from the individual simulations equal to no more than ±17 cms.

A dynamic response to the coupled interaction of climate and LULC was observed for the sediment loading and nonlinearities resulting from the coupling of climate and LULC change were more identifiable for the A2 and B1 scenarios while A1B remained relatively linear (Figure 5d–f). All models indicated sediment increase may be amplified by the coupled interaction when both climate only and LULC only simulations predicted an increase (October A2—HADCM3, November A1B—IPCM4, and August A2—MPEH5). When both climate and LULC were predicted to decrease from the baseline independently (April B1—MPEH5 and June B1—HADCM3), the combined interaction caused less of a decrease from the baseline than would be estimated by adding the deviation quantities from the two individual simulations. In an instance when the loading for LULC only decreased and climate only increased (March A1B—HADCM3), sediment loads may result in larger values compared with the linear response. Conversely, when LULC only increased and climate only decreased (April A2—MPEH5 and February A2—IPCM4) loadings may be predicted as having overall smaller values than expected if the incremental increase/decrease from the baseline for isolated climate and LULC change simulations were added.

5. Discussion

Climate change predicted by the individual GCMs showed noticeable differences in future rainfall seasonal patterns with no one-carbon emission scenario resulting in higher values, emphasizing the structural differences among GCMs. The general consensus for temperature is that it will increase, with the A2 scenario predicting the highest values and B1 predicting the lowest. When incorporating climate change into the SWAT model, output in terms of runoff and sediment loading showed large distinctions between GCMs, implying that these parameters might have been driven more by rainfall than temperature. Both the runoff and sediment loading responded to future climate change, yet, the ways in which they responded may be conflicting between GCMs. Under present conditions, high flows occur around October–December. Results from all GCMs are in agreement that flow increased for the months of September and October, indicating the current wet season may occur earlier in the year and with greater magnitude. In accompaniment, sediment loadings were also predicted to increase for these months. Further, loading for the baseline was at its minimum from July to September, yet, a seasonal shift may occur with minimal loading occurring earlier in the year, around April to June. This response may be driven by the lowered future precipitation that occurs within these months.

LULC change had little effect on the runoff response. Surface runoff was computed using the SCS curve number method. While the individual curve number values assigned to the distinct land classes varied within the model, the weighted, cumulative curve numbers for the circa 2000, 2100 A2, A1B, and B1 land cover datasets within the study domain were 46.9, 48.7, 45.7, and 44.4. The slight variability between curve number values might explain why runoff was so minimally affected by LULC change. An alternative future LULC class assignment than that used in this study may result in a more significant response. Further, response to alterations in LULC may be more appropriately assessed using a finer temporal resolution capable of addressing peak runoff. The slight increase that does occur from August to October for the A2 scenario land cover might be explained by the plant growth model and consequent evapotranspiration that is incorporated into SWAT.

Sediment loading was more evidently impacted by changes made to land cover than runoff. The loading increase observed from the A2 LULC may be a result of the increase in agricultural lands and loss of forested area. Sediment loading decreased for all months as a result of the B1 coverage. Compared with the circa 2000 coverage, B1 had more forested regions and less agriculture. It is inferred that the amount of agricultural and forested lands was directly related to sediment loading and that an increase in agriculture and/or loss of forest may have caused loading quantities to increase.

Runoff response for simulations that coupled climate and LULC change produced runoff values that were very similar to those produced by incorporating climate change only, suggesting that future climate change may affect flow more than LULC change. Regardless of the behavior of increased or decreased runoff predicted by the individual models, the patterns of amplification and de-amplification were alike, demonstrating a homogenous interaction occurring within the simulations that was not affected by the GCM data. Sediment loading response was more reactive. When climate and LULC both independently modeled sediment as increasing or as decreasing, the coupled response resulted in sediment values that were overall larger than would be estimated from the individual, added deviations from the baseline. This suggests climate and LULC change effects amplify one another, resulting in larger loadings than if estimated by the separately modeled responses.

Many of the species in the Apalachicola region are sensitive to salinity and total suspended solids levels, which can affect both their productivity and distributions [*Livingston*, 1984; *Scavia et al.*, 2002]. The increase in high flow magnitude and seasonal shifts for runoff and sediment caused by climate change has implications for threatening the phenology of the system by affecting migration, breeding, and distributions. In addition, as land types change, adverse effects may become amplified. Given the time horizon of this study, results may provide guidance in establishing both short and long monitoring activities and mitigation strategies. Short-term efforts may focus on responses with less uncertainty, i.e., those in agreement among all GCM. Long-term strategies, with more flexibility to adapt, can help coastal managers to adjust sustainability efforts and regulatory procedures as more knowledge is acquired, e.g., how the region is changing and region-specific performance of GCMs. The suite of SRES scenarios provides yet another dimension to adaptation planning.

Understanding of how certain land types affect hydrologic processes is useful for future land use planning initiatives and development, in Apalachicola and other fluvial estuaries. As coastal regions become more urbanized and land types continue to change, the potential for increased sediment loading should be considered by policy makers and coastal managers.

As part of the AFC River Basin, insight for how the Apalachicola region might respond under potential future conditions may guide practices upstream. In particular, it may have relevance for planned drainage and infrastructure improvements that increase water returns and help to guide minimum flow regulation at the Jim Woodruff Lock and Dam.

Findings from this study are significant to future modeling approaches. The nonlinear response when modeling climate and LULC change advocates subsequent modeling efforts should include the two simultaneously. Output response differed among the SRES scenarios produced by a particular GCM. Climate change assessments using only one scenario may over or under predict impacts and simulating multiple scenarios may be advantageous to develop a suite of equipotential outcomes. Lastly, this research addresses overland processes, an essential component for integrated climate change vulnerability assessments. Results may serve as inputs or boundary conditions for studies evaluating SLR, marsh productivity, coastal erosion, etc.

6. Conclusions

For this study, a hydrologic SWAT model was developed, calibrated, and validated for the Apalachicola River Basin under historical conditions. Projected climate and LULC data were prepared to represent future conditions related to the IPCC SRES A2, A1B, and B1 scenarios for 2100. The datasets were assimilated into the model to assess the responses of runoff and sediment loading to changes in climate, LULC, and coupled climate and LULC.

Findings from this research showed differing behaviors for both runoff and sediment loading predicted by the GCMs and SRES scenarios. The variability in response to the implemented GCMs further advocate the

use of multi-model ensembles and additional research is needed to determine region-specific performance of individual GCMs to better optimize model ensembles and eliminate erroneous outputs.

Despite contrasting outputs among the individual GCMs, all models converge on the following points, which may serve to guide management focus. The models indicate that climate change may induce seasonal shifts that could extend or completely alter periods of high and low runoff and sediment loading. Peak runoff was predicted to occur earlier in the year, around September and October, and minimum sediment loading also occurred earlier in the year, around April and June, as compared to present day conditions. The simulated seasonal shifts in runoff and sediment have implications for affecting the phenology of the ecosystem. Runoff response to changes in LULC was minimal, however, an alternative LULC classification scheme different than that used in this study may result in a more significant reaction. Larger sediment loading was associated with increased agriculture, increased urban areas, and decreased forested regions. A nonlinear response was observed when climate and LULC change were incorporated in the model simulation simultaneously, implying changes in one may amplify or dampen the effects of the other. The dynamic interaction that exists suggests that both should be incorporated into hydrologic models when studying future conditions. Differing responses among the SRES scenarios indicate that it may be advantageous to include multiple scenarios for future climate change assessments to provide coastal managers with a suite of equally varying outcomes that can be used for developing mitigation strategies.

The results from this study provide an improved understanding of the effects of climate and LULC change on water quantity and quality for the Apalachicola Bay and surrounding region as well as similar fluvial estuaries. The outcomes can better guide management practices that may pertain to regulatory actions, land use development and planning, and monitoring activities. Future studies may address the assumptions held constant or omitted for this study including changes in hydrology and land use upstream the Jim Woodruff Lock and Dam, human activities, e.g., future consumptive demand, dynamic response of habitats, e.g., marsh migration, and freshwater-sea interaction, e.g., SLR impacts. The outputs from this research will be used in biological assessments as boundary conditions and inputs for models studying the ecology of this system, e.g., marshes, oysters, and seagrasses. One study will use a hydro-marsh model to assess salt marsh productivity in the Apalachicola River region under present and future scenarios that consider projected changes in climate, LULC, and SLR. The IPCC carbon emission scenarios used in this study will be linked to low, intermediate low, intermediate high, and high SLR scenarios [*Parris et al.*, 2012]. Another study will incorporate the streamflow and sediment loading under projected climate and LULC change into a circulation model that will be used to study how freshwater and sediments are distributed into Apalachicola Bay and the ways in which seagrasses are affected.

Acknowledgments

The authors would like to thank K. Schenter at the U.S. Army Corps of Engineers Mobile District for providing the surveyed bathymetry, the Apalachicola National Estuarine Research Reserve for their helpful cooperation, and X. Chen for providing data and insight. We also thank M. Hooshyar, Y. Tang, D. Sandhu, X. Han, and the anonymous reviewers for their constructive comments. All data for this paper are properly cited and referred to in the reference list.

References

Asselman, N. E. M. (2000), Fitting and interpretation of sediment rating curves, *J. Hydrol.*, *234*(3–4), 228–248, doi:10.1016/s0022-1694(00)00253-5.

Asselman, N. E. M., H. Middelkoop, and P. M. v. Dijk (2003), The impact of change in climate and land use on soil erosion, transport and deposition of suspended sediment in the River Rhine, *Hydrol. Processes*, *17*(16), 3225–3244, doi:10.1002/hyp.1384.

Benaman, J., C. A. Shoemaker, and D. A. Haith (2005), Calibration and validation of soil and water assessment tool on an agricultural watershed in upstate New York, *J. Hydrol. Eng.*, *10*(5), 363–374, doi:10.1061/asce1084-0699200510:5363c.

Bilskie, M. V., S. C. Hagen, K. Alizad, S. C. Medeiros, D. L. Passeri, H. Needham, and A. Cox (2016), Dynamic simulation of numerical analysis of hurricane storm surge under sea level rise along the northern Gulf of Mexico, *Earth's Future*, doi:10.1002/2015EF000347.

Butcher, J. B., T. E. Johnson, D. Nover, and S. Sarker (2014), Incorporating the effects of increased atmospheric CO_2 in watershed model projections of climate change impacts, *J. Hydrol.*, *513*(26), 322–334, doi:10.1016/j.jhydrol.2014.03.073.

Cai, X., D. Wang, T. Zhu, and R. Claudia (2009), Assessing the regional variability of GCM simulations, *Geophys. Res. Lett.*, *36*(2), L02706, doi:10.1029/2008GL036443.

Caldwell, P. V., et al. (2015), A comparison of hydrologic models for ecological flows and water availability, *Ecohydrology*, *8*(8), 1525–1546, doi:10.1002/eco.1602.

Chen, J., X. Li, and M. Zhang (2005), Simulating the impacts of climate variation and land-cover changes on basin hydrology: a case study of the Suomo basin, *Sci. China Earth Sci.*, *48*(9), 1501–1509, doi:10.1360/03yd0269.

Chen, X., K. Alizad, D. Wang, and S. C. Hagen (2014), Climate change impact on runoff and sediment loads to the Apalachicola River at seasonal and event scales, *J. Coastal Res.*, *68*, 35–42, doi:10.2112/sl68-005.1.

Couch, C. A., E. H. Hopkins, and P. S. Hardy (1996), Influences of environmental settings on aquatic ecosystems in the Apalachicola-Chattahoochee-Flint River Basin, *Rep. 95-4278*, U.S. Geol. Surv., Atlanta, Ga.

Dibike, Y. B., and P. Coulibaly (2005), Hydrologic impact of climate change in the Saguenay watershed: comparison of downscaling methods and hydrologic models, *J. Hydrol.*, *307*(1–4), 145–163, doi:10.1016/j.jhydrol.2004.10.012.

Easterling, D. R., G. A. Meehl, C. Parmesan, S. A. Changnon, T. R. Karl, and L. O. Mearns (2000), Climate extremes: observations, modeling, and impacts, *Science*, *289*(5487), 2068–2074, doi:10.1126/science.289.5487.2068.

Ficklin, D. L., Y. Luo, E. Luedeling, and M. Zhang (2009), Climate change sensitivity assessment of a highly agricultural watershed using SWAT, *J. Hydrol.*, *374*(1–2), 16–29, doi:10.1016/j.jhydrol.2009.05.016.
Gassman, P. W., M. R. Reyes, C. H. Green, and J. G. Arnold (2007), The soil and water assessment tool: historical development, applications, and future research directions, *Trans. ASABE*, *50*(4), 1211–1250, doi:10.13031/2013.23637.
Georgakakos, A., F. Zhang, and H. Yao (2010), Climate varibility and change assessment for the ACF river basins, *Rep. Technical Report No. GWRI/2010-TR1*, 321 pp., Georgia Water Resour. Inst. (GWRI), Atlanta, Ga.
Gibson, C. A., J. L. Meyer, N. L. Poff, L. E. Hay, and A. Georgakakos (2005), Flow regime alterations under changing climate in two river basins: implications for freshwater ecosystems, *River Res. Appl.*, *21*(8), 849, doi:10.1002/rra.855.
Gupta, H., S. Sorooshian, and P. Yapo (1999), Status of automatic calibration for hydrologic models: comparison with multilevel expert calibration, *J. Hydrol. Eng.*, *4*(2), 135–143, doi:10.1061/(asce)1084-0699(1999)4:2(135).
Hay, L. E., S. L. Markstrom, and C. Ward-Garrison (2011), Watershed-scale response to climate change through the twenty-first century for selected basins across the United States, *Earth Interact.*, *15*(17), 1–37, doi:10.1175/2010el370.1.
Intergovernmental Panel on Climate Change (2000), Special reports: emissions scenarios, *Rep.*, IPCC, UK.
Intergovernmental Panel on Climate Change (2007), Climate change 2007: the physical science basis, *Rep.*, 966 pp., IPCC, Cambridge, UK and New York.
Intergovernmental Panel on Climate Change (2013), Climate change 2013: the physical science basis. Contribution of working group I, *Rep.*, 1535 pp., Intergovernmental Panel on Clim. Change, Cambridge, UK and New York.
Intergovernmental Panel on Climate Change (2014a), Scenario process overview, in *Scenario Process for AR5*, Intergovernmental Panel on Clim. Change. [Available at http://sedac.ipcc-data.org/ddc/ar5_scenario_process/scenario_overview.html.]
Intergovernmental Panel on Climate Change (2014b), Synthesis report: contribution of working groups I, II and III to the Fifth Assessment report of the Intergovernmental Panel on Climate Change, *Rep.*, 151 pp., IPCC, Geneva, Switzerland.
Isphording, W. C. (1986), Apalachicola Bay: dynamic sedimentation in a Gulf Coast estuary, *Gulf Coast Assoc. Geol. Soc. Trans.*, *36*, 471–488.
Jha, M. K., and P. W. Gassman (2014), Change is hydrology and streamflow as predicted by a modelling experiment forced with climate models, *Hydrol. Processes*, *28*(5), 2772–2781, doi:10.1002/hyp.9836.
Johnson, T. E., J. B. Butcher, A. Parker, and C. P. Weaver (2012), Investigating the sensitivity of U.S. streamflow and water quality to climate change: U.S. EPA Global Change Research Program's 20 Watersheds Project, *J. Water Resour. Plann. Manage.*, *138*(5), 453–464, doi:10.1061/(asce)wr.1943-5452.0000175.
Johnson, T., et al. (2015), Modeling streamflow and water quality sensitivity to climate change and urban developments in 20 U.S. watersheds, *J. Am. Water Resour. Assoc.*, *51*(5), 1321–1341, doi:10.1111/1752-1688.12308.
Karl, T. R., and R. W. Knight (1998), Secular trends of precipitation amount, frequency, and intensity in the United States, *Bull. Am. Meteorol. Soc.*, *79*, 231–241, doi:10.1175/1520-0477(1998)079<0231:stopaf>2.0.CO;2.
Krysanova, V., and R. Srinivasan (2015), Assessment of climate and land use change impacts with SWAT, *Reg. Environ. Change*, *15*, 431–434, doi:10.1007/s10113-014-0742-5.
Lambin, E. F., et al. (2001), The causes of land-use and land-cover change: moving beyond the myths, *Global Environ. Change*, *11*(4), 261–269, doi:10.1016/s0959-3780(01)00007-3.
Livingston, R. J. (1984), The ecology of the Apalachicola Bay system: an estuarine profile, *Rep.*, 148 pp., U.S. Fish Wildlife Serv, Tallahassee, Fla.
Martin, J. F., E. Reyes, P. Kemp, H. Mashriqui, and J. W. J. Day (2002), Landscape modeling of the Mississippi delta, *BioScience*, *52*(4), 357–365, doi:10.1641/0006-3568(2002)052[0357:lmotmd]2.0.CO;2.
Mearns, L. O., F. Giorgi, P. Whetton, D. Pabon, M. Hulme, and M. Lal (2004), Guidelines for use of climate scenarios developed from regional climate model experiments, *Rep.*, Data Distrib. Cent. of the Intergovernmental Panel on Clim. Change. [Available at http://www.ipcc-data.org/guidelines/dgm_no1_v1_10-2003.pdf.]
Menne, M. J., I. Durre, R. S. Vose, B. E. Cleason, and T. G. Houston (2012), An overview of the global historical climatology network-daily database, *J. Atmos. Oceanic Technol.*, *29*, 897–910, doi:10.1175/jtech-d-11-00103.1.
Milly, P. C. D., J. Betancourt, M. Falkenmark, R. M. Hirsch, Z. W. Kundzewicz, D. P. Lettenmaier, and R. J. Stouffer (2008), Stationarity is dead: whither water management? *Science*, *319*(5863), 573–574, doi:10.1126/science.1151915.
Monteith, J. L. (1965), Evaporation and environment, in *Symposia of the Society for Experimental Biology*, pp. 205–223, Cambridge Univ. Press, Cambridge, U. K.
Moriasi, D. N., J. G. Arnold, M. W. V. Liew, R. L. Bingner, R. D. Harmel, and T. L. Veith (2007), Model evaluation guidelines for systematic quantification of accuracy in watershed simulations, *Trans. ASABE*, *50*(3), 885–900, doi:10.13031/2013.23153.
Narsimlu, B., A. K. Gosain, and B. R. Chahar (2013), Assessment of future climate change impacts on water resources of Upper Sind River Basin, India using SWAT model, *Water Resour. Manage.*, *27*(10), 3647–3662, doi:10.1007/s11269-013-0371-7.
Nash, J. E., and J. V. Sutcliffe (1970), River flow forecasting through conceptual models part I – a discussion of principles, *J. Hydrol.*, *10*(3), 282–290, doi:10.1016/0022-1694(70)90255-6.
National Centers for Environmental Prediction (2016), *Climate Forecast System Reanalysis*, Data Support Section of the Computational and Information Systems Laboratory at the National Center for Atmospheric Research, Boulder, Colo. [Available at http://rda.ucar.edu/pub/cfsr.html.]
National Climate Assessment (2014), Climate change impacts in the United States: the third National Climate Assessment, *Rep.*, 841 pp., U.S. Global Change Research Program, Washington, D. C.
Neitsch, S. L., J. G. Arnold, J. R. Kiniry, and J. R. Williams (2011), Soil and water assessment tool theoretical documentation, *Rep. 406*, USDA Agric. Res. Serv. (ARS) Grassland, Soil and Water Res. Lab., Texas Agric. Exp. Stn., Blackland Res. Cent., Temple, Tex.
Ogdena, N. H., A. Maaroufc, I. K. Barkerd, M. Bigras-Poulina, L. R. Lindsaye, M. G. Morshedf, C. J. O'Callaghang, F. Ramayh, D. Waltner-Toewsh, and D. F. Charronb (2006), Climate change and the potential for range expansion of the Lyme disease vector *Ixodes scapularis* in Canada, *Int. J. Parasitol.*, *36*(1), 63–70, doi:10.1016/j.ijpara.2005.08.016.
Pal, I., B. T. Anderson, G. D. Salvucci, and D. J. Gianotti (2013), Shifting seasonality and increasing frequency of precipitation in we and dry seasons across the U.S., *Geophys. Res. Lett.*, *40*(15), 4030–4035, doi:10.1002/GRL.50760.
Pan, S., G. Li, Q. Yang, Z. Ouyang, G. Lockaby, and H. Tian (2013), Monitoring Land-Use and Land-Cover Change in the Eastern Gulf Coastal Plain Using Multi-temporal Landsat Imagery, *J. Geophys. Remote Sensing*, *2*, 108, doi:10.4172/2169-0049.1000108.
Park, J.-Y., M.-J. Park, S.-R. Ahn, G.-A. Park, J.-E. Yi, G.-S. Kim, R. Srinivasan, and S.-J. Kim (2011), Assessment of future climate change impacts on water quantity and quality for mountainous dam watershed using SWAT, *Trans. ASABE*, *54*(5), 1725–1737, doi:10.13031/2013.39843.
Parris, A., et al. (2012), Global sea level rise scenarios for the US National Climate Assessment, *Rep.*, 37 pp., Climate Program Office, Silver Spring, Md.

Passeri, D. L., S. C. Hagen, S. C. Medeiros, M. V. Bilskie, K. Alizad, and D. Wang (2015), The dynamic effects of sea level rise on low-gradient coastal landscapes: a review, *Earth's Future*, *3*, 159–181, doi:10.1002/2015EF000298.
Passeri, D. L., S. C. Hagen, N. G. Plant, M. V. Bilskie, S. C. Medeiros, and K. Alizad (2016), Tidal hydrodynamics under future sea level rise and coastal morphology in the northern Gulf of Mexico, *Earth's Future*, *4*, doi:10.1002/2015EF000332.
Phan, D. B., C. C. Wu, and S. C. Hsieh (2011), Impact of climate change on stream discharge and sediment yield in northern Viet Nam, *Water Resour.*, *38*(6), 827–836, doi:10.1134/s0097807811060133.
Plant, N. G., E. R. Thieler, and D. L. Passeri (2016), Coupling centennial-scale shoreline change to sea-level rise and coastal morphology in the Gulf of Mexico using a Bayesian network, *Earth's Future*, *4*, doi:10.1002/2015EF000331.
Praskievicz, S., and H. Chang (2009), A review of hydrological modelling of basin-scale climate change and urban development impacts, *Prog. Phys. Geogr.*, *33*(5), 650–671, doi:10.1177/0309133309348098.
Richardson, C. W. (1981), Stochastic simulation of daily precipitation, temperature, and solar radiation, *Water Resour. Res.*, *17*(1), 182–190, doi:10.1029/WR017I001P00182.
Saleh, A., and B. Du (2004), Evaluation of SWAT and HSPF within basins program for the Upper North Bosque River watershed in central Texas, *Trans. ASABE*, *47*(4), 1039–1049, doi:10.13031/2013.16577.
Sathiamurthy, E. (2013), Potential effect of sea level rise on Rambai river, Malaysia, *World Appl. Sci.*, *22*(3), 359.
Scavia, D., et al. (2002), Climate change impacts on U.S. Coastal and Marine Ecosystems, *Estuaries*, *25*(2), 149–164, doi:10.1007/bf02691304.
Schilling, K. E., M. K. Jha, Y.-K. Zhang, P. W. Gassman, and C. F. Wolter (2008), Impact of land use and land cover change on the water balance of a large agricultural watershed: historical effects and future directions, *Water Resour. Res.*, *44*(7), W00A09, doi:10.1029/2007WR006644.
Schilling, K. E., K.-S. Chan, H. Lui, and Y.-K. Zhang (2010), Quantifying the effect of land use land cover change on increasing discharge in the Upper Mississippi River, *J. Hydrol.*, *387*(3–4), 343–345, doi:10.1016/j.jhydrol.2010.04.019.
Seaber, P. R., F. P. Kapinos, and G. L. Knapp (1987), Hydrologic unit maps: U.S. Geological Survey Water-Supply, *Rep.*, 63 pp. [Available at http://water.usgs.gov/GIS/huc.html.]
Semadeni-Davies, A., C. Hernebring, G. Svensson, and L.-G. Gustafsson (2008), The impacts of climate change and urbanisation on drainage in Helsingborg, Sweden: suburban stormwater, *J. Hydrol.*, *350*, 114–125, doi:10.1016/j.jhydrol.2007.11.006.
Semenov, M. A., and E. M. Barrow (1997), Use of a stochastic weather generator in the development of climate change scenarios, *Clim. Change*, *35*, 397–414, doi:10.1023/a:1005342632279.
Semenov, M. A., and R. J. Brooks (1999), Spatial interpolatin of the LARS-WG stochasitc weather generator in Great Britain, *Clim. Res.*, *11*, 137–148, doi:10.3354/cr011137.
Semenov, M. A., and P. Stratonovitch (2010), Use of multi-model ensembles from global climate models for assessment of climate change impacts, *Clim. Res.*, *41*, 1–14, doi:10.3354/cr00836.
Semenov, M. A., R. J. Brooks, E. M. Barrrow, and C. W. Richardson (1998), Comparison of WGEN and LARS-WG stochastic weather generators for diverse climates, *Clim. Res.*, *10*, 95–107, doi:10.3354/cr010095.
Shi, P.-J., Y. Yuan, J. Zheng, J.-A. Wang, Y. Ge, and G.-Y. Qiu (2007), The effect of land use/cover change on surface runoff in Shenzhen region, China, *CATENA*, *69*(1), 31–35, doi:10.1016/j.catena.2006.04.015.
Shrestha, B., M. S. Babel, S. Maskey, A. v. Griensven, S. Uhlenbrook, A. Green, and I. Akkharath (2013), Impact of climate change on sediment yield in the Mekong River basin: a case study of the Nam Ou basin, Lao PDR, *Hydrol. Earth Syst. Sci.*, *17*, 1–20, doi:10.5194/hess-17-1-2013.
Singh, J., H. V. Knapp, and M. Demissie (2005), Hydrological modeling of the iroquois river watershed using HSPF and SWAT, *J. Am. Water Resour. Assoc.*, *41*(2), 343–360, doi:10.1111/j.1752-1688.2005.tb03740.x.
Soil Conservation Service (1972), Section 4: hydrology, *National engineering handbook*, *Rep.*, Soil Conserv. Serv., Washington, D.C.
Srinivasan, R., and J. G. Arnold (1994), Integration of a basin-scale water quality model with GIS, *J. Am. Water Resour. Assoc.*, *30*(3), 453–462, doi:10.1111/j.1752-1688.1994.tb03304.x.
Tóth, B., and E. Bódis (2015), Estimation of suspended loads in the Danube River at Göd (1668 river km), Hungary, *J. Hydrol.*, *523*, 139–146, doi:10.1016/j.jhydrol.2015.01.031.
Tuppad, P., K. R. Douglas-Mankin, T. Lee, R. Srinivasan, and J. G. Arnold (2011), Soil and Water Assessment Tool (SWAT) hydrologic/water quality model: extended capability and wider adoption, *Trans. ASABE*, *54*(5), 1677–1684, doi:10.13031/2013.39856.
U.S. Environmental Protection Agency (2013), Watershed modeling to assess the sensitivity of streamflow, nutrient, and sediment loads to potential climate change and urban development in 20 U.S. watersheds, *Rep. EPA/600/R-12/058F*, Natl. Cent. Environ. Assess., Washington, D.C.
United States Department of Agriculture (2007), *Soil Survey Geographic Database*, edited by U.S. Department of Agriculture, USDA, Washington, D.C.
United States Geological Survey (2001), *National Water Information System in Water Data for the Nation*, U.S. Department of the Interior and U.S. Geological Survey. [Available at http://waterdata.usgs.gov/nwis/uv?site_no=02358000.]
United States Geological Survey (2012), *Surface-Water Annual Statistics for Florida*, U.S. Department of the Interior and U.S. Geological Survey. [Available at http://waterdata.usgs.gov/fl/nwis/sw.]
United States Geological Survey (2013a), *USGS NED 1/3 Arc-Second 2013 1 × 1 Degreee ArcGRID*, U.S. Geol. Surv., Reston, Va..
United States Geological Survey (2013b), *Federal standards and procedures for the national Watershed Boundary Dataset (WBD), in* Chapter 3 of Section A, Federal Standards Book 11, Collection and Delineation of Spatial Data, U.S. Geol. Surv. and the U.S. Dep. Agric. [Available at http://pubs.usgs.gov/tm/11/a3/.]
USGS EROS Center (2014), *CONUS Modeled Annual Land-Cover Maps of the A1B, A2, and B1 Scenario From 2006–2100*, U.S. Dep. Interior, U.S. Geol. Surv. [Available at http://landcover-modeling.cr.usgs.gov/projects.php.]
Valentim, J. M., L. Vaz, N. Vaz, H. Silva, B. Duarte, I. Cacador, and J. M. Dias (2013), Sea level rise impact in residual circulatino in Tagus estuary and Ria de Aveiro lagoon, *J. Coastal Res.*, *2*(65), 1981–1986, doi:10.2112/sI65-335.1.
Vogelmann, J. E., S. M. Howard, L. Yang, C. R. Larson, B. K. Wylie, and J. N. V. Driel (2001), Completion of the 1990's national land cover data set for the conterminous United States, *Photogramm. Eng. Remote Sens.*, *67*, 650–662.
Walling, D. E. (1974), Suspended sediment and solute yields from a small catchment prior to urbanization, in *Fluvial Processes in Instrumented Watersheds* , edited by K.J. Gregory and D.E. Walling, pp. 169–192, Institute of British Geographers, London.
Wang, D., and M. Hejazi (2011), Quantifying the relative contribution of the climate and direct human impacts on mean annual streamflow in the contiguous United States, *Water Resour. Res.*, *47*, W00J12, doi:10.1029/2010WR010283.

Wang, D., S. C. Hagen, and K. Alizad (2013), Climate change impact and uncertainty analysis of extreme rainfall events in the Apalachicola River basin, Florida, *J. Hydrol.*, *480*, 125–135, doi:10.1016/j.jhydrol.2012.12.015.

Wang, R., L. Kalin, W. Kuang, and H. Tian (2014), Individual and combined effects of land use/cover and climate change on Wolf Bay watershed streamflow in southern Alabama, *Hydrol. Processes*, *28*, 5530–5546, doi:10.1002/hyp.10057.

Ward, P. J., R. T. v. Balen, G. Verstraeten, H. Renssen, and J. Vandenberghe (2009), The impact of land use and climate change on late Holocene and future suspended sediment yield of the Meuse catchment, *Geomorphology*, *103*(3), 389–400, doi:10.1016/j.geomorph.2008.07.006.

Wilby, R. L. (1997), Non-stationarity in daily precipitation series: implication for GCM down-scaling using atmospheric circulation indices, *Int. J. Climatol.*, *17*, 439–454, doi:10.1002/(sici)1097-0088(19970330)17:4<439::aid-joc145>3.0.co;2-u.

Wilby, R. L., and T. M. L. Wigley (1997), Downscaling general circulation model output: a review of methods and limitations, *Prog. Phys. Geogr.*, *21*(4), 530–548, doi:10.1177/030913339702100403.

Wilby, R. L., T. M. L. Wigley, D. S. Wilks, B. C. Hewitson, D. Conway, and P. D. Jones (1996), Statistical downscaling of general circulation model output, *Rep.*, Palo Alto, Calif.

Williams, J. R. (1995), Chapter 25: the EPIC model, in *Computer Models of Watershed Hydrology*, edited by V. P. Singh , pp. 909–1000 , Water Resour. Publ., Highlands Ranch, Colo.

Yan, B., N. F. Fang, P. C. Zhang, and Z. H. Shi (2013), Impacts of land use change on watershed streamflow and sediment yield: an assessment using hydrologic modelling and partial least squares regression, *J. Hydrol.*, *484*, 26–37, doi:10.1016/j.jhydrol.2013.01.008.

Zhang, X., R. C. Izaurrald, J. G. Arnold, J. R. Williams, and R. Srinivasan (2013), Modifying the soil and water assessment tool to simulation cropland carbon flux: model development and initial evaluation, *Sci. Total Environ.*, *463–464*, 810–832, doi:10.1016/j.scitotenv.2013.06.056.